Results in Physics 3 (2013) 161–166

Contents lists available at ScienceDirect

Results in Physics

journal homepage: www.journals.elsevier.com/results-in-physics

Numerical study of Williamson nano fluid flow in an asymmetric channel

Noreen Sher Akbar [a,*], S. Nadeem [b], Changhoon Lee [c], Zafar Hayat Khan [d], Rizwan Ul Haq [b]

[a] DBS&H, CEME, National University of Sciences and Technology, Islamabad, Pakistan
[b] Department of Mathematics, Quaid-i-Azam University 45320, Islamabad 44000, Pakistan
[c] Department of Computational Science and Engineering, Yonsei University, Seoul, South Korea
[d] School of Mathematical Sciences, Peking University, Beijing 100871, PR China

ARTICLE INFO

Article history:
Received 29 June 2013
Accepted 20 August 2013
Available online 2 September 2013

Keywords:
Peristaltic flow
Numerical solutions
Nano particle phenomena
Asymmetric channel
Williamson fluid

ABSTRACT

This article investigates with the peristaltic flow of a Williamson nano fluid in an asymmetric channel. The related modeling of the problem has been done in Cartesian coordinate system. Problem has been simplified with the reliable assumptions i.e. long wave length and small Reynolds number. Numerical solutions have been evaluated for stream function, velocity profile, temperature profile, nano particle phenomena and pressure rise. Graphical results have been presented and discussed for various involved parameters.

1. Introduction

Peristalsis is an instinctive movement of the longitudinal and circular muscles, mostly in the digestive tract but infrequently in other hollow tubes of the body, that occur in progressive wave like contractions. This mechanism occurs in the esophagus, stomach, and intestines. The waves can be short, local reflexes or long, continuous contractions that travel the whole length of the organ, depending upon their location and what initiates their action. Mekheimer and Elmaboud [1] discussed the influence of heat transfer and magnetic field on peristaltic transport of a Newtonian fluid in a vertical annulus. In another article Mekheimer [2] presented the induced magnetic field effects on the peristaltic flow of a couple stress fluid in a channel. S. Gayathri and Kothandapani in their combined work quoted [3–5] the influence of heat and mass transfer, wall properties and slip conditions for Newtonian fluid. Mathematical model for the peristaltic flow of chyme movement in small intestine is given by Tripathi [6]. He [7] also discussed the peristaltic transport of fractional Maxwell fluids in uniform tubes with endoscopy applications. Very recently, Akber et al. [8] presented the Williamson fluid model for the peristaltic flow in an inclined asymmetric channel with partial slip and heat transfer.

Nanoparticle research is currently an area of intense scientific interest due to a wide variety of potential applications in biomedical, optical and electronic field. In nanotechnology, a particle is defined as a small object that behaves as a whole unit in terms of its transport and properties. Particles are further classified according to size in terms of diameter, coarse particles cover a range between 10,000 and 2,500 nm. Fine particles are sized between 2,500 and 100 nm. The term "nanofluid" was first coined by Choi [9] which refers to a conventional heat transfer fluid (Water, Oil, ethylene glycol, etc) containing a dispersion of nanosize particles. The basic idea is to use the nanoparticles as a tool enhancing the thermal conductivities of the base fluids. For more detail see Refs. [10–24].

The current study discusses the peristaltic flow of a Williamson nano fluid in an asymmetric channel. The governing equations have been modeled in Cartesian coordinate system and simplified by employing reliable approximations and assumptions. The numerical solution of stream function, longitudinal pressure gradient, temperature profile, nanoparticle phenomena and pressure rise has been calculated. Graphical results have been presented in order to illustrate the variations of involved parameters.

2. Mathematical formulation

We discussed an incompressible magnetohydrodynamic (*MHD*) Williamson nano fluid in an asymmetric channel. The width of

* Corresponding author.
E-mail address: noreensher@yahoo.com (N.S. Akbar).

2211-3797
http://dx.doi.org/10.1016/j.rinp.2013.08.005

Table 1
Numerical values of velocity profile for $x = 1$, $a = 0.1$, $d = 1$, Nb = 0.5, Nt = 0.5, Br = 2, Gr = 2, $M = 1$, $Q = 2$, $\phi = 0.4$, We = 0.1, $b = 0.5$.

↓y	$u(x, y)$	↓y	$u(x, y)$	↓y	$u(x, y)$
−1.10	−1.00000	−0.39	0.37996	0.39	0.21386
−1.00	−0.673642	−0.29	0.40866	0.49	0.11727
−0.89	−0.39331	−0.19	0.41759	0.59	−0.0223
−0.79	−0.16820	−0.09	0.41157	0.69	−0.32589
−0.69	−0.01008	0.09	0.38835	0.89	−0.54135
−0.59	0.14866	0.19	0.34800	0.99	−0.80312
−0.49	0.32922	0.29	0.29018	1.10	−1.00000

Table 2
Numerical values of pressure rise ΔP for $a = 0.1$, $d = 1$, Nb = 0.5, Nt = 0.5, Br = 2, Gr = 2, $M = 1$, $\phi = 0.4$, We = 0.1, $b = 0.5$.

↓Q	ΔP	↓Q	ΔP	↓Q	ΔP
−3	6.66131	−1.0	2.48383	1	−1.68666
−2.5	5.61677	−0.5	1.44020	1.5	−2.72711
2	4.57226	0	0.39714	2	−3.76639
−1.5	3.52790	0.5	−0.64519	2.5	−4.80432

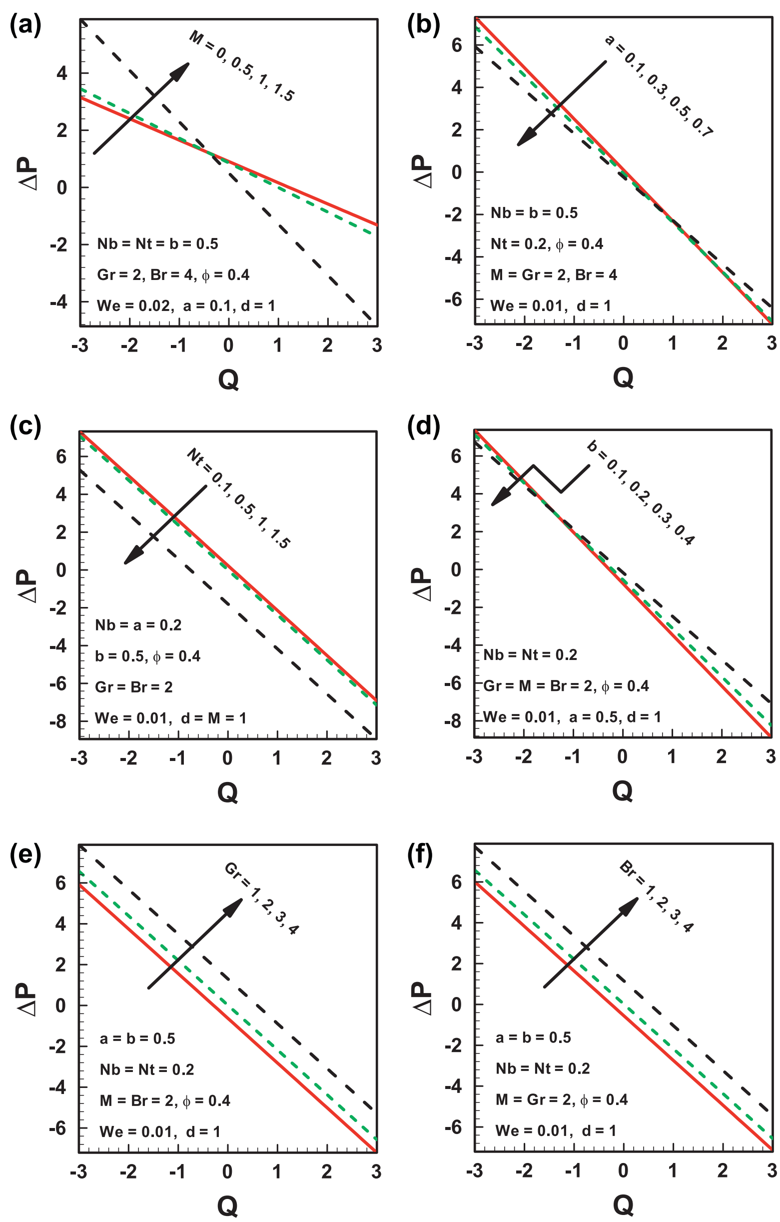

Fig. 1. Variation of pressure rise versus flow rate for M, a, Nt, We, Gr, Br.

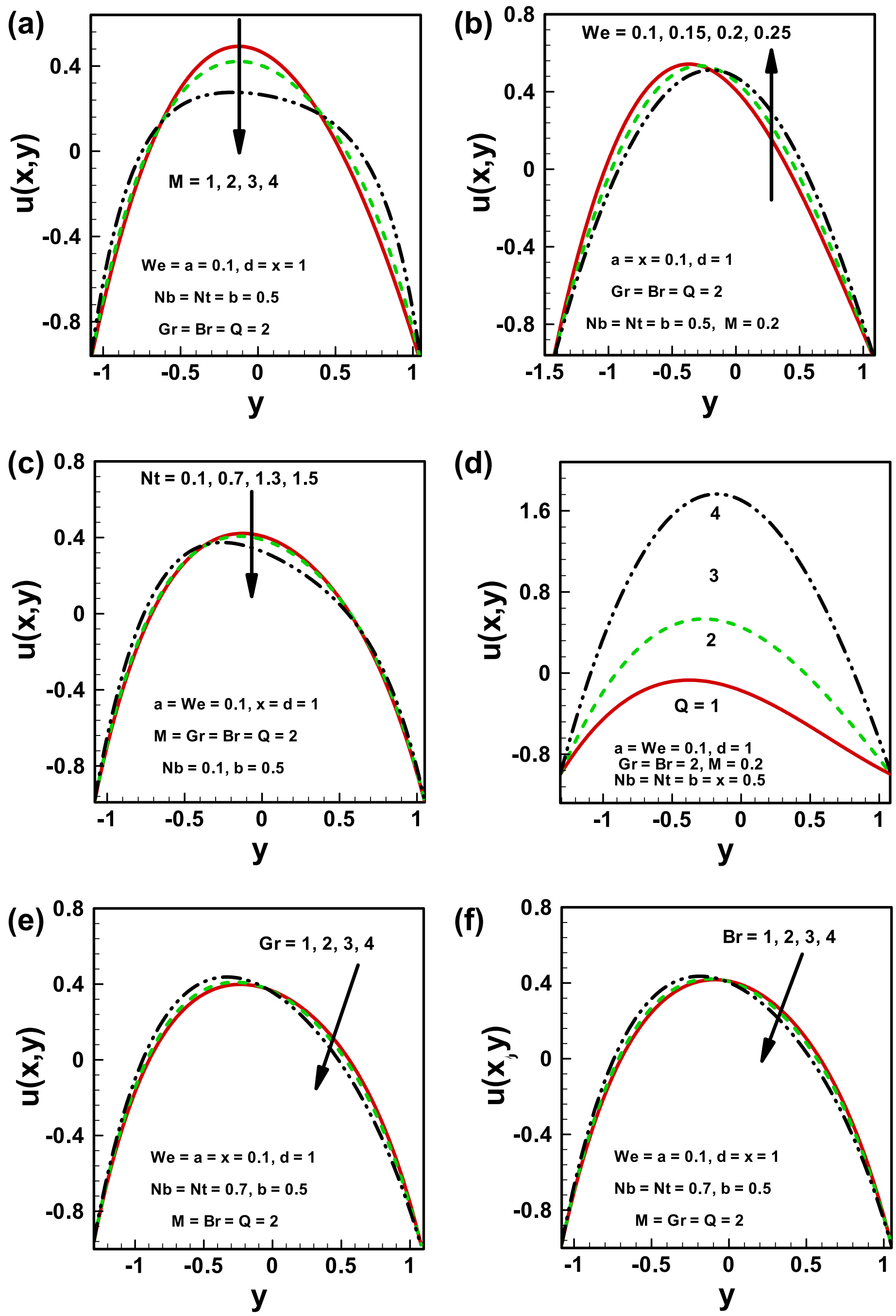

Fig. 2. Variation of velocity profile for M, We, Q, Nt, Gr and Br.

channel is taken as $d_1 + d_2$. Flow is induced due to sinusoidal wave propagating with constant speed c on the channel walls. The heat transfer analysis with nanoparticle is maintained by giving temperatures T_0 and T_1 to the lower and upper walls of a channel correspondingly. The wall surfaces are taken as

$$Y = H_1 = d_1 + a_1 \cos\left[\frac{2\pi}{\lambda}(X - ct)\right],$$
$$Y = H_2 = -d_2 - b_1 \cos\left[\frac{2\pi}{\lambda}(X - ct) + \phi\right], \tag{1}$$

in above equations a_1 and b_1 are the wave amplitudes, λ is the wave length, $d_1 + d_2$ is the channel width, c is the wave speed, t is the time, X is the direction of wave propagation and Y is perpendicular to X. The phase difference ϕ varies in the range $0 \leqslant \phi \leqslant \pi$. For $\phi = 0$ the symmetric channel with waves out of phase can be described and when $\phi = \pi$, the waves are in phase. Moreover, a_1, b_1, d_1, d_2 and ϕ fulfill the following relation

$$a_1^2 + b_1^2 + 2a_1 b_1 \cos\phi \leqslant (d_1 + d_2)^2.$$

The transformations between the laboratory and wave frames are given by

$$x = X - ct, \; y = Y, \; u = U - c, \; v = V, \; p(x) = P(X, t). \tag{2}$$

The stream function Ψ is defined by

$$u = \frac{\partial \Psi}{\partial y}, \; v = -\delta \frac{\partial \Psi}{\partial x} \tag{3}$$

which satisfies the continuity equation identically.

Dimensionless variables are defined by

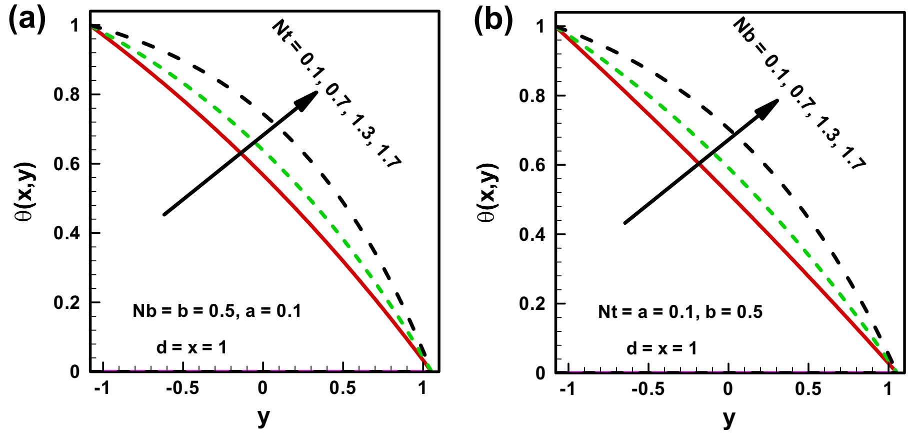

Fig. 3. Variation of temperature profile for *Nt* and *Nb*.

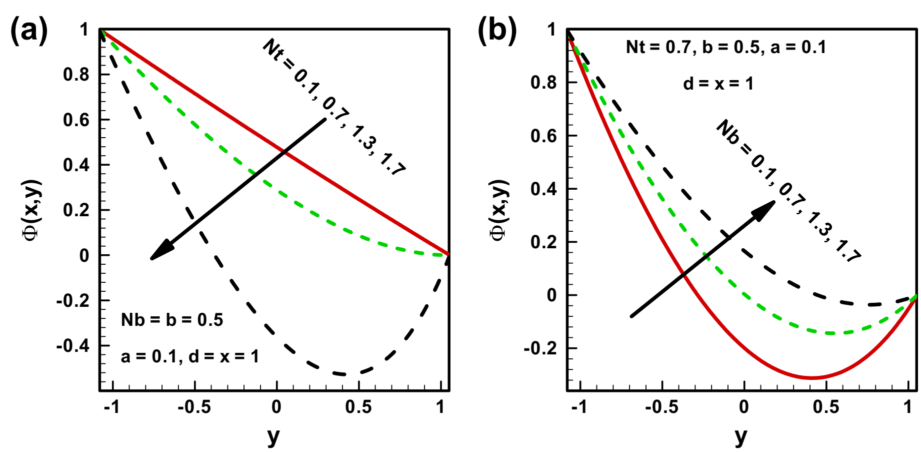

Fig. 4. Variation of nano particle phenomena for *Nt* and *Nb*.

$$x = \frac{2\pi\bar{x}}{\lambda},\ y = \frac{\bar{y}}{d_1},\ u = \frac{\bar{u}}{c_1},\ v = \frac{\bar{v}}{c_1},\ t = \frac{2\pi\bar{t}}{\lambda},\ \delta = \frac{2\pi d_1}{\lambda},\ d = \frac{d_2}{d_1},\ P = \frac{2\pi d_1^2\bar{P}}{\mu c_1\lambda},$$
$$h_1 = \frac{\bar{h}_1}{d_1},\ h_2 = \frac{\bar{h}_2}{d_2},\ Re = \frac{\rho c_1 d_1}{\mu},\ a = \frac{a_1}{d_1},\ b = \frac{a_2}{d_1},\ d = \frac{d_2}{d_1},\ S = \frac{\bar{S}d_1}{\mu c_1},$$
$$\theta = \frac{\bar{T}-\bar{T}_0}{\bar{T}_1-\bar{T}_0},\ \Phi = \frac{\bar{C}-\bar{C}_0}{\bar{C}_1-\bar{C}_0},\ \alpha = \frac{k}{(\rho c)_f},\ Nb = \frac{(\rho c)_p D_B(\bar{C}_1-\bar{C}_0)}{(\rho c)_f\alpha},\ P_r = \frac{\nu}{\alpha},$$
$$Nt = \frac{(\rho c)_p D_{\bar{T}}(\bar{T}_1-\bar{T}_0)^2}{\bar{T}_0(\rho c)_f\alpha},\ Gr = \frac{g\alpha d_1^2(\bar{T}_1-\bar{T}_0)}{\nu c_1},\ Br = \frac{g\alpha d_1^2(\bar{C}_1-\bar{C}_0)}{\nu c_1},$$
$$We = \frac{\Gamma c}{d_1},\ M = \sqrt{\frac{\sigma}{\mu}}B_0 d_1. \tag{4}$$

The flow equations for Williamson fluid in dimensionless form under long wave length and low Reynold's number approximation take the form [6]

$$\frac{\partial^2}{\partial y^2}\left[\frac{\partial^2\Psi}{\partial y^2} + We\left(\frac{\partial^2\Psi}{\partial y^2}\right)^2 - M^2\Psi\right] + Gr\frac{\partial\theta}{\partial y} + Br\frac{\partial\sigma}{\partial y} = 0, \tag{5}$$

$$\frac{dP}{dx} = \frac{\partial}{\partial y}\left[\frac{\partial^2\Psi}{\partial y^2} - M^2\Psi + We\left(\frac{\partial^2\Psi}{\partial y^2}\right)^2\right] + Gr\theta + Br\sigma, \tag{6}$$

$$\frac{\partial^2\theta}{\partial y^2} + P_r Nb\frac{\partial\theta}{\partial y}\frac{\partial\Phi}{\partial y} + P_r Nt\left(\frac{\partial\theta}{\partial y}\right)^2 = 0, \tag{7}$$

$$\frac{\partial^2\Phi}{\partial y^2} + \frac{Nt}{Nb}\left(\frac{\partial^2\theta}{\partial y^2}\right) = 0, \tag{8}$$

in above equations P_r, Nb, Nt, Gr and Br denote respectively the Prandtl number, the Brownian motion parameter, the thermophoresis parameter, local temperature Grashof number and local nanoparticle Grashof number.

The corresponding boundary conditions can be put into the following forms:

$$\Psi = \frac{F}{2},\ \frac{\partial\Psi}{\partial y} = -1,\ \theta = 1,\ \Phi = 1,\ at\ y = h_1 = 1 + a\cos x, \tag{8a}$$

$$\Psi = -\frac{F}{2},\ \frac{\partial\Psi}{\partial y} = -1,\ \theta = 0,\ ,\ \Phi = 0,\ at\ y = h_2 = -d - b\cos(x+\varphi), \tag{8b}$$

Expression relating the time mean flow rate F (in the fixed frame) and Q (in the wave frame) is

$$Q = F + 1 + d. \tag{9}$$

and the expression for dimensionless pressure rise ΔP is

$$\Delta P = \int_0^1\left(\frac{dP}{dx}\right)dx. \tag{10}$$

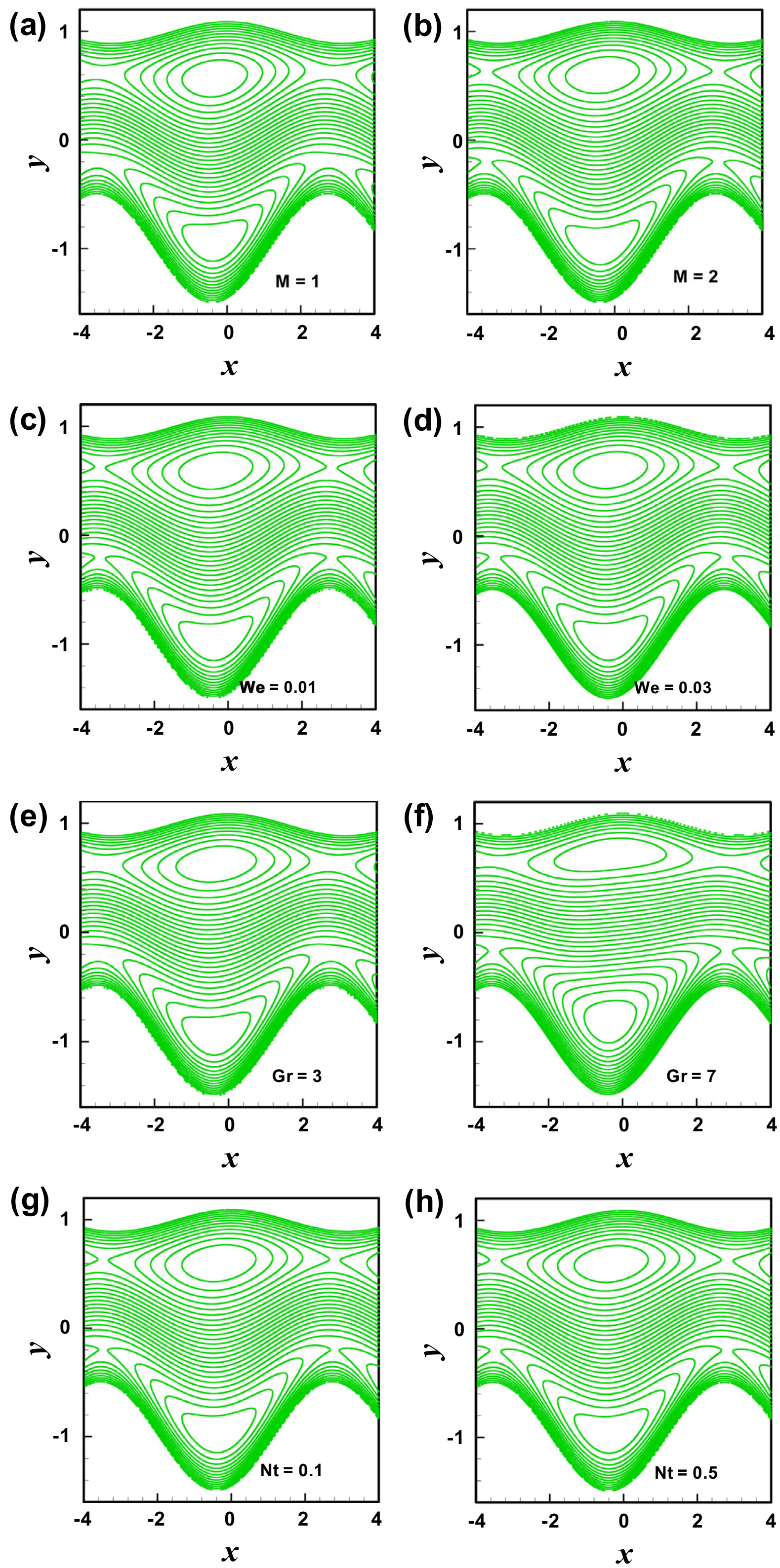

Fig. 5. Stream lines for panels ((a) and (b)) for M = 1, 2, ((c) and (d)) for We = 0.01, 0.02, ((e) and (f)) for Gr = 2, 3, ((g) and (h)) for Nt = 0.5, 0.7, while the others parameters are $a = 0.1$, $d = 1$, Nb = 0.4, Br = 0.5, $\phi = 0.4$, $b = 0.5$.

3. Results and discussion

The resulting nonlinear differential Eqs. (5)–(8) with Eqs. (8a), (8b) have been solved numerically by using Maple 16, the fourth and fifth order Runge–Kutta–Fehlberg method is used to build the numerical scheme. This section describes the numerical results graphically for pressure rise, velocity, temperature and streamlines. The pressure rise per wavelength has been examined through graphs. The pressure rise against volume flow rate is shown in Fig. 1(a)–(f). Basically the pressure rise and volume flow rate have opposite results. Fig. 1a–f shows that in pumping region ($\Delta P > 0$), the pressure rise increases when Hartman number M, thermophoresis parameter Nt, local temperature Grashof number Gr and local nanoparticle Grashof number Br increase and augmented pumping occurs for ($\Delta P < 0$). Figs. 1a–f depict that the pressure rise decreases by increasing the Hartman number M, thermophoresis parameter Nt, local temperature Grashof number Gr and local nanoparticle Grashof number Br. The free pumping region corresponds to ($\Delta P = 0$). Variations of Hartman number M, Weissenberg number We and flow rate Q on the velocity profile are shown in Fig. 2(a)–(f). Fig. 2(a) shows that the velocity near the channel walls is not similar in view of the Hartman number M. The velocity decreases by increasing M. The velocity for the Weissenberg number has been plotted in Fig. 2(b). It is found that the velocity field increases in the region $y \in [-1.5, 0]$, where as it decreases in the region $y \in [0.1, 1]$ when the Weissenberg number We increases. Fig. 2(c) depicts that an increase in flow rate Q increases the velocity field. Influence of thermophoresis parameter Nt, local temperature Grashof number Gr and local nanoparticle Grashof number Br on velocity profile is shown in Fig. 2(a)–(f). It is analyzed that the velocity field decreases in the region $y \in [-1.5,0]$, where as it increases in the region $y \in [0.1,1]$ when Nt, Gr, and Br increase. The variation in temperature profile for different values of Brownian motion parameter Nb and thermophoresis parameter Nt are plotted in Fig. 3(a) and (b). Here the temperature profile increases when Brownian motion parameter Nb and the thermophoresis parameter Nt increase. Nanoparticle phenomena have been shown graphically in Fig. 4(a) and (b). It is seen that nanoparticle phenomena decreases with increase in Brownian motion parameter Nb and increases when we increase thermophoresis parameter Nt.

The trapping for different values of M, We, Gr and Nt is shown in Fig. 5(a)–(h). It is seen from Fig. 5(a–d) that the size of the trapping bolus increases by increasing M and We (in the upper and lower parts of the channel). Fig. 5e–h presents that the size and number of the trapping bolus decrease with an increase in Gr and Nt (in the upper and lower parts of the channel). Table 1 and table 2 gives the numerical values of velocity and pressure rise.

References

[1] Mekheimer Kh S, Abd Elmaboud Y. Influence of heat transfer and magnetic field on peristaltic transport of a Newtonian fluid in a vertical annulus. Application of an endoscope. Phys Lett A 2008;372:1657–65.

[2] Mekheimer Kh S. Effect of the induced magnetic field on peristaltic flow of a couple stress fluid. Phys Lett A 2008;372:4271–8.

[3] Srinivas S, Gayathri R. Peristaltic transport of a Newtonian fluid in a vertical asymmetric channel with heat transfer and porous medium. Appl Math Comput 2009;180:2115–22.

[4] Srinivas S, Gayathri R, Kothandapani M. The influence of slip conditions, wall properties and heat transfer on MHD peristaltic transport. Comput Phys Commun 2009;180:2115–22.

[5] Srinivas S, Kothandapani M. The influence of heat and mass transfer on MHD peristaltic flow through a porous space with compliant walls. Appl Math Comput 2009;213:197–208.

[6] Tripathi D. Mathematical model for the peristaltic flow of chyme movement in small intestine. Math Biosci 2011;233:90–7.

[7] Tripathi D. Peristaltic transport of fractional Maxwell fluids in uniform tubes: applications in endoscopy. Comput Math Appl 2011;62:1116–26.

[8] Akbar NS, Nadeem S, Hayat T, Obaidat S. Peristaltic flow of a Williamson fluid in an inclined asymmetric channel with partial slip and heat transfer. Int J Heat Mass Transfer 2012;55:1855–62.

[9] Choi SUS. Enhancing thermal conductivity of fluids with nanoparticles. In: Siginer DA, Wang HP, editors. Developments and Applications of Non-Newtonian Flows. New York: ASME; 1995. p. 99–105.

[10] Buongiorno J. Convective transport in nanofluids. ASME J Heat Transfer 2006;128:240–50.

[11] Khanafer K, Vafai K, Lightstone M. Buoyancy-driven heat transfer enhancement in a two-dimensional enclosure utilizing nanofluids. Int J Heat Mass Transfer 2003;46:3639–53.

[12] Das Sarit K, Putra Nandy, Roetzel Wilfried. Pool boiling of nano-fluids on horizontal narrow tubes. Int J Multiphase Flow 2003;29:1237–47.

[13] Kuznetsov AV, Nield DA. Natural convective boundary-layer flow of a nanofluid past a vertical plate. Int J Ther Sci 2010;49:243–7.

[14] Makinde OD, Aziz A. Boundary layer flow of a nanofluid past a stretching sheet with a convective boundary condition. Int J Ther Sci 2011;50:1326–32.

[15] Aziz A, Khan WA. Natural convective boundary layer flow of a nanofluid past a convectively heated vertical plate. Int J Thermal Sci 2012;52:83–90.

[16] Akbar Noreen Sher, Nadeem S, Hayat T, Hendi Awatif A. Peristaltic flow of a nano fluid with slip effects. Meccanica 2012;47:1283–94.

[17] Akbar Noreen Sher, Nadeem S. Endoscopic effects on the peristaltic flow of a nanofluid. Commun Theor Phys 2011;56:761–8.

[18] Akbar Noreen Sher, Nadeem S, Hayat T, Hendi Awatif A. Peristaltic flow of a nanofluid in a non-uniform tube. Heat Mass Transfer 2012;48:451–9.

[19] Akbar Noreen Sher, Nadeem S, Hayat T, Hendi Awatif A. Peristaltic flow of a nanofluid with slip effects. Meccanica 2012;47:1283–94.

[20] Akbar Noreen Sher, Nadeem S. Peristaltic flow of a Phan-Thien-Tanner nanouid in a diverging tube. Heat Transfer Res 2012;41:10–22.

[21] Hosseinzadeh H, Dehghan M, Mirzaei D. The boundary elements method for magneto-hydrodynamic (MHD) channel flows at high Hartmann numbers. Appl Math Model 2013;37:2337–51.

[22] Khan ZH, Khan W, Pop I. Triple diffusive free convection along a horizontal plate in porous media saturated by a nanofluid with convective boundary condition. Int J Heat Mass Tran 2013;66:603–12.

[23] Shakeri F, Dehghan M. A finite volume spectral element method for solving magnetohydrodynamic (MHD) equations. Appl Numer. Math 2011;61:1–23.

[24] Dehghan M, Mirzaei D. Meshless local boundary integral equation (LBIE)method for the unsteady magnetohydrodynamic (MHD) flow in rectangular and circular pipes. Comp Phys Commun 2009;180:1458–66.